EVALUATING THE INFLUENCE OF CHAIN BRANCHING ON THE ADHESION STRENGTH BETWEEN LAYERS IN FUSED DEPOSITION MODELING

EVALUATING THE INFLUENCE OF CHAIN BRANCHING ON THE ADHESION STRENGTH BETWEEN LAYERS IN FUSED DEPOSITION MODELING

By

Mohammed T. Alturkestany, B. ENG

A Thesis
Submitted to the School of Graduate Studies
in Partial Fulfillment of the Requirements for the Degree
Master of Applied Science

McMaster University

Master of Applied Science (2017)
McMaster University
(Chemical Engineering) Hamilton, Ontario

TITLE: Influence of Chain Branching on the Adhesion Strength between Layers in Fused Deposition Modeling

AUTHOR: Mohammed T. Alturkestany
B. ENG (McMaster University)

SUPERVISOR: Dr. Michael Thompson

NUMBER OF PAGES: VIII - 45

Lay Abstract

Fused Deposition Modeling (FDM) is a recent popular method of plastic 3D printing technique, in which plastic filament is heated to a molten state to be then deposited through a layer-by-layer fashion to successfully fabricate parts. One of the drawbacks of that technology is the low bonding strength developed between layers as compared to strength along the length direction of layers. This study focuses on developing a testing methodology to evaluate the adhesion strength between layers and altering the material structure to maximize such strength. Four types of polylactic acid with different degrees of chain branching were successfully processed, printed and tested. Material with higher degree of branching yielded higher adhesion strength.

Abstract

Fused deposition modeling (FDM) is gaining an ever increasing attention for its ability to fabricate complex geometry parts and prototypes at lower cost. The technology is striving to produce parts with high mechanical resistance that can withstand and perform under high stress environment. The adhesion strength between layers, transverse strength, is a limiting factor that need to be quantitatively evaluated to further understand and improve the bonding behavior of thermoplastic polymer in FDM. This interfacial adhesion is derived by the diffusion and penetration of polymer chains across the interface allowing the chain entanglement to form a bonding medium.

This study investigates the bonding behaviour of polylactic acid (PLA) as a function of chain branching. The adhesion strength is quantitatively evaluated by developing and performing a peel test of a two-printed layer samples. It is possible to increase chain branching of PLA by bulk modification with epoxy chain extender. The modification of PLA was carried out using an internal batch mixer with four different concentrations of chain extender. The modified PLA was processed into print filament and characterized by parallel plate rheometry and DSC.

It was found that the addition of chain extender increased molecular weight and degree of branching of PLA and in return the peel testing results reflected a significant increase in adhesion strength. Such improvement can be attributed to the long branched chains of

PLA and its ability to create entanglements between layers. These findings can help in producing better PLA filaments to provide a higher stress resistance for FDM fabricated functional parts.

ACKNOWLEDGMENTS

I would like to acknowledge my supervisor Dr. Michael Thompson for his continues support, guidance, discussions and encouragement throughout the course of this research.

I would also like to express my thanks to the Saudi Arabian Cultural Bureau for the funding provided for this research and all the support put out to help me complete this work.

I would like to thank Elizabeth Takacs for the training provided to use the lab instruments. Also, my thanks go to Paul Gatt for his technical support in designing and putting together the apparatus required for this study.

I would like to express my deepest thanks and appreciation to my parents, brother Mansoar, and sisters for the love and support they have been blessing me with throughout my academic journey.

Last but certainly not the least, I would like to acknowledge my gratitude to my fiancée Ghdeer for all the love, encouragement and inspiration she has been to me.

Contents

List of Tables

List of Figures

Chapter 1. Introduction

The technology of 3D printing has been gaining a lot of attention over the past few years [1]. It has proven successful by providing solutions for different applications and improving performance of products from industries such as pharmaceutical, automotive and manufacturers. The *fused deposition modeling* (FDM) technique went from use only in fabricating prototypes to producing fully functional parts that are reliable, as well as cost and time effective.

A FDM process uses thermoplastic polymer filament to deposit layer-by-layer on the print bed from bottom to top to create the shape communicated by the software. Such software takes a CAD drawing and slice it into a set number of layers, usually 0.2-0.4 mm in height. It communicates how to print these layers along with operating instruction such as layering orientation, temperature, and print speed in G-code format. Each deposited line of material is called a *road* or *bead*, and deposition of multiple roads adjacent to each other is called a *layer*.

Despite the increasing popularity of FDM systems, the technology is still facing many challenges. Strength of the finished part, print speed, material and print size limitations are preventing the technology from stepping into a mass production phase. Lower strength parts corresponds to the lack of sufficient layer-to-layer adhesion, however, different research have been evaluating the different parameters and conditions to increase adhesion. Average print speed is anywhere between 30-50 mm/s, with some printers capable of printing up to 150 mm/s without compromising quality. Printing at higher speed will

notably cause a significant drop in quality due to filament slippage [2]. Increasing efforts are being devoted to developing compatible FDM materials, with over 30 commercial types of filaments available in order to draw the attention of different industries and consumers. [3]

A wide range of thermoplastic materials are used in FDM for different needs and applications. There have been numerous types of materials developed for use in FDM. These materials include *acrylonitrile butadiene styrene* (ABS), *polylactic acid* (PLA) [4], *Nylon*, *Polycarbonate* (PC) and *Polyethylene terephthalate* (PET). Each material is generally rated according to strength, flexibility, and stability properties related to heat, chemical and weather resistance. Some have been rated for medical and food safety such as *polyethylene-terephthalate-glycol* ETG and PLA.

Polylactic acid (PLA) is one of the most used FDM filaments due to different factors, some of which are its biodegradable nature, quality of print and minimal fume release. However, it lacks the level of strength that ABS exhibits, which makes it less favorable for high performance mechanical parts. However, different grades/blends of PLA have been developed for higher strength properties. [3]

PLA is an aliphatic polyester made by the polymerization of lactic acid ($C_3H_6O_3$), which is derived from renewable natural feedstocks such as corn and sugarcane. There is an ever increasing demand for PLA in recent years to compete in replacing traditional petroleum derived plastics in applications such as packaging and disposable items; such demand is continuously reducing the cost of PLA. According to leading producers, global production of PLA will reach 1 million tonnes by 2020. [5]

Research Objective

The scope of this research is focused on understanding the effect of molecular weight (Mw) on the adhesion strength between any two printed layers of PLA. Our hypothesis is that increasing M_w of PLA can enhance the entanglements between layers, thus increasing strength in the transverse direction of printed specimens.

Evaluation of strength between two layers is achieved here by performing a peel test, where the energy required to separate two printed layers is measured against the length of the sample. Such results are expected to provide an understanding on the nature of bonding strength created between layers rather than along each layer. Increasing strength between layers would result in stronger part, especially strength in the direction perpendicular to the FDM print bed. Different PLA grades were developed for this study using different chain extension (Joncryl) concentrations and processed into 3D print filament to be printed into a rectangular shape samples consisting of two layers.

Chapter 2. Literature review

2.1 Overview

With the increasing popularity of FDM technology and its applications, a considerable amount of research and study has been conducted to evaluate properties and test for variations. Fabrication of FDM parts depends on a set of variables that dictate the end results. Major variables in FDM that influence quality of print are temperature, layer thickness and orientation of print.

Some research focused on evaluating surface roughness of printed objects and optimized print conditions to increase surface smoothness such that layers were as indistinguishable as possible. The objective was to produce surface finishes similar to those of injection molding. Others have looked into assessing material warping to minimize and prevent deformation in printed parts.

On the other hand, the majority of FDM research is based on evaluating the mechanical properties of printed specimens and quantifying the effects of different controllable parameters. A number of studies examined the tensile strength as a function of layer orientation (i.e raster angle). Varying the raster angle changes the direction of beads with respect to the part build orientation, see Figure **1**. Similarly, layer thickness and part porosity (air gaps) were other key factors to improving strength.

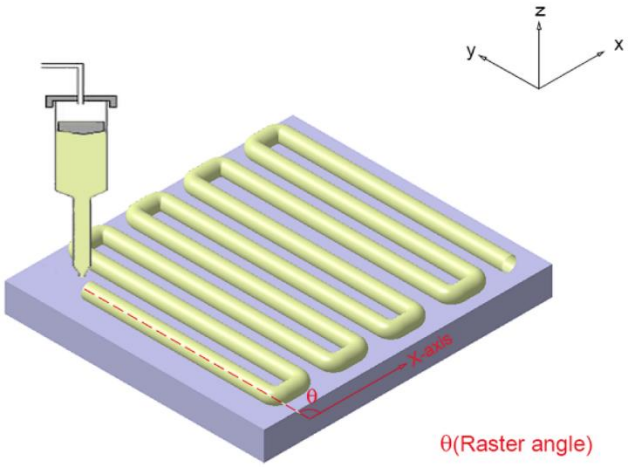

Figure 1:Raster angle depiction, shown above raster angle of 90° (transverse) orientation. [6]

In addition, various experimentation with different materials, mainly PLA and ABS, have provided a clear material guideline for the different mechanical characterizations. PLA is a brittle material and is more prone to break when bent (i.e., brittle fracture), but nevertheless it makes a suitable material for its print quality and biocompatibility. Printing with ABS has been shown to present different challenges.

The following sections describe the current research in the areas of printer operation and material properties focused on improving the mechanical performance of printed objects.

2.2 FDM Technology

Fused deposition modeling (FDM), this technology was first patented by Scott Crump in 1989, a co-founder of Stratasys Inc. It was not until the past recent years that the technology has surfaced and drew attention from developers and manufacturers. Different open source software were developed to provide printing standard guide that beginners can follow to obtain desired print quality.

The printing process consist of three main parts, material in use, extrusion head mechanics, and communication code. There is no need for dies or special tools to create the desired shape, if it can be drawn it can be printed, Figure **2** outlines FDM process. Depending on the purpose from each print, material selection is important to provide the characterization needed, top two materials in use are ABS and PLA. The thermoplastic filament is fed to the extrusion head typically via feeding gear, to be melt and deposited on the build platform. It is important that extrusion head is capable of supplying and maintain print temperature, 165^{o}C (PLA), 210-230^{o}C (ABS) and up to 270^{o}C for nylon.

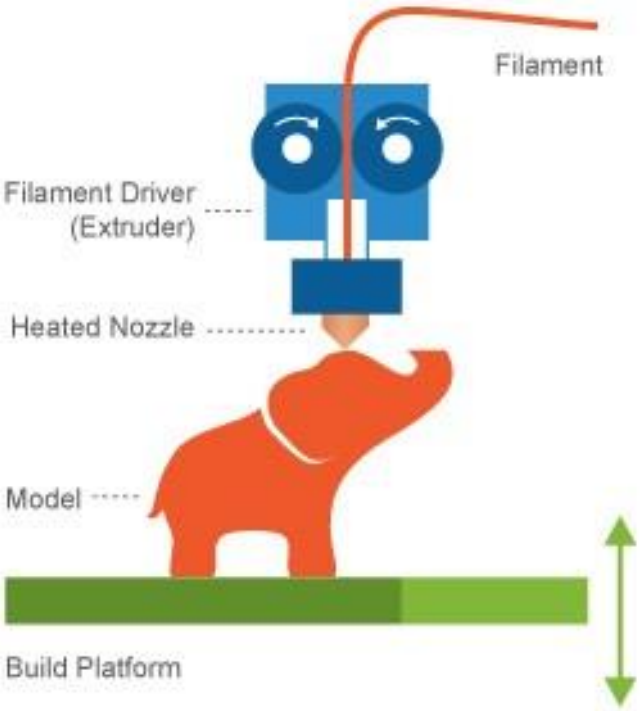

Figure 2:illustration of FDM process [7]

All print specifications are selected through the slicing software i.e., Slic3r, where parameters such as temperature, layer thickness, perimeters, layering orientation and fill density is specified. Each parameter influence build time, resolution and strength of the part. Larger layer thickness would decrease print time but also reduce print quality and resolution. Fill density of 100% would yield stronger parts and uses more material to complete the printing job. Depending on the strength required of the part, fill density and fill pattern can be modified to meet the balance between material used, time consumed and overall strength. Once all parameters are selected through the slicing software, communication code is created in G-code format.

Interface software (Printer Host), verity of different software packages are available to serve this purpose i.e., Repetier, Pronterface, and Cura. This host software initiates communication to the printer and transmit commands from G-code generated. The part is fabricated layer-by-layer, heated nozzle deposits beads of molten filament and movement of print head is achieved through step motors. X and Y-axis movement directions is used to trace 2D shape of each layer, after each layer is complete, Z-axis movement takes place to elevate for the proceeding layer.

2.3 Mechanical Properties

Ziemain et al. [8] studied the influence of print orientation and directionality of the polymer molecules on the tensile strength of ABS. Fabricating dog-bone specimen by FDM allowed for fair comparison of mechanical properties to injection molding. The tensile stress values reported were 93% and 34% for axial and transverse, respectively, compared to that of injection molding. They found that tensile strength by printing exclusively in the

longitudinal direction significantly exceeded that using a transverse orientation. Huang et al. [9] observed similar results by performing a tensile test with ABS. They found samples prepared using a transverse print orientation to have only 32.6% tensile strength of those prepared with a longitudinal print orientation. They also tested samples with raster angle of 15^{o}, 30^{o}, 45^{o}, 75^{o} which yielded 94.8%, 83.4%, 59.2%, 43.7% and 37.6% of the maximum tensile strength. These results indicate the significant influence of raster angles on the mechanical properties of printed objects. Ahn et al. [10] examined the effect of different print parameters on specimen strength printed with ABS. They varied the parameters of raster angle, bead width (BW), print temperature (PT), color and air-gap (AG) between beads. They concluded BW and PT to have a negligible effect on strength. Specimens printed with a longitudinal raster angle (i.e., 0^{o}) displayed significantly larger tensile strength compared to those printed with a transverse raster angle (i.e., 90^{o}). Reducing the AG from 0.00 to -0.003mm (i.e., over-lap of beads) improved the overall tensile strength for printed specimens with either raster orientation. Compressive strength was also examined and showed higher values for longitudinal specimens.

Christiyan et al. [11] investigated the effect of layer thickness and print speed on tensile strength. An ABS/ hydrous silicate composite was used as the print material and samples were prepared by varying layer thickness (0.2, 0.25 and 0.3 mm) and print speed (30, 40 and 50 mm/s). Maximum tensile strength values were reported for samples printed with 30 mm/s and layer thickness of 0.2mm, showing favour for higher density printing of beads to improve mechanical properties. Similarly, Wu et al. [6] examined the effect of layer thickness on tensile strength with *Polyether-ether-ketone* (PEEK). Three samples printed

with a raster angle of 0^o and layer thickness of 0.2, 0.3, or 0.4mm were tested. The resulted tensile strength was respectively 40.1, 56.6 and 32.4 MPa, indicating high dependence on layer thickness. Their results suggested that the average tensile strength of PEEK samples was 108% higher than that of ABS, while compressive strength and bending strength were 118% and 115% greater than that of ABS. The two studies above show optimal layers thickness to produce greater mechanical strength is dependent on material selection.

2.4 PLA Syntheses

Among the different renewable and bio-degradable materials available, PLA polymer is preferred for most applications [12]. It is easily processed on conventional polymer equipment and produced in films, fibers and molded parts [13]. The natural degradation time of PLA falls anywhere between six months to two year, and it breaks down to carbon dioxide and water, compared to oil based polymers which last 500 years (i.e., polystyrene, polyethylene) [14].

The first recorded syntheses of PLA were in 1845 by Theophile-Jules Pelouze and in 1932, Wallace Carothers who successfully polymerized lactide into PLA and then went on to patent the polymer with Du Pont in 1954 [15, 16]. At that time, the PLA produced had low molecular weight and was limited to pharmaceutical applications. It was not until the mid-1990's, when Cargill Inc. (now trading as NatureWork) successfully polymerized high molecular weight poly(L-lactic acid) (PLLA) by ring opening polymerization (ROP) of L- Lactide, cyclic L-dimer of lactic acid [15,17].

Lactic acid, the building blocks of PLA, has two stereoisomers L-lactic acid and D-lactic acid. Lactide forms from the condensation of these two lactic acid (LA) molecules,

yielding either L-lactide, D-lactide, or meso-lactide, which is the condensation result of two L-LA, D-LA or L,D-LA respectively. Chemical structure of lactic acid and lactide is shown in Figure **3.**

Behaving similar to polyethylene terephthalate (PET), the molecular weight of PLA can be readily modified by hydrolysis or chain extension reactions.

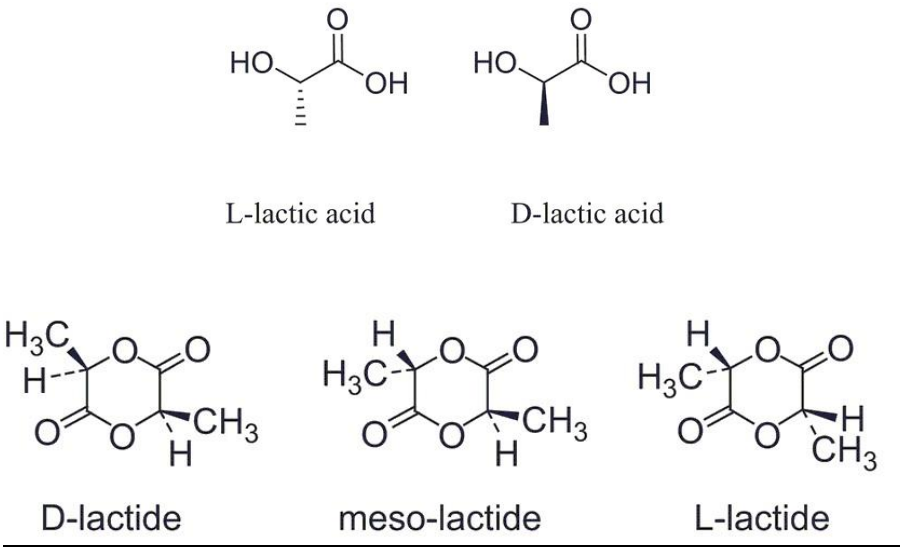

Figure 3: Chemical structure of L-,D-lactic acid, L-,D-,meso-lactide.[18]

2.4.1 Chain Extender Effect

The ring-opening polymerization of lactide yields high molecular weight PLA, but it is relatively complicated and expensive [19, 20]. PLA obtained from direct condensation reaction has a low molecular weight, which is increased by chain extenders to make it desirable for different applications. Chain extenders are chemical compounds used to react with the functional end groups of a polymer chain, which are carboxyl and hydroxyl species for PLA chain, to bridge the chains together. Reported increases in molecular weight of PLA due to effect of branching, see a corresponding increase in melt viscosity,

ductility, and overall strength while crystallinity is reduced [20,21]. The different common methods of producing PLA are outlined in Figure 4.

Joncryl® (BASF) is an example of chain extension technology that produces non-linear polymer chains. It is an epoxy-functional styrene-acrylic or styrene-free acrylic based reactive polymer, which has been shown to significantly improve mechanical, rheological and physical properties of PLA while maintaining optical properties [22]. Pilla et al. used Joncryl to improve melt strength of PLA during extrusion and injection molding. Oza et al. studied the effect of acrylic based chain extenders, including Joncryl, and found it to be the most effective in improving melt viscosity of PLA/starch blend. Najafi et al. observed an increase in molecular weight of PLA by reacting 1 wt% of Joncryl with PLA in an internal mixer for 11 min at 190^{o}C [23].

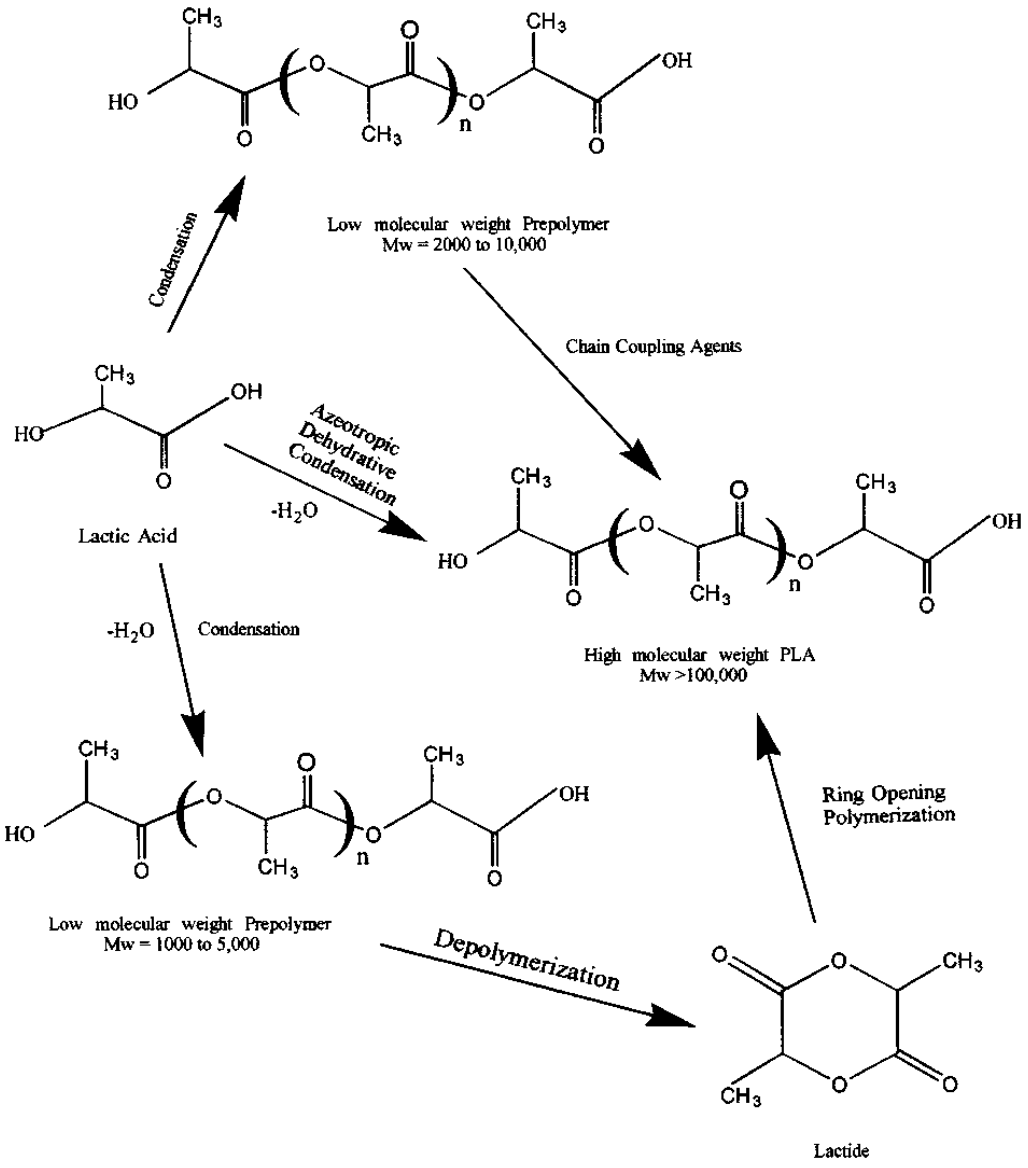

Figure 4:Methods of PLA synthesis [19]

Chapter 3. Experimental Methods

3.1 Raw Material

The PLA used for this study was NatureWork^{TM} PLA 7000D purchased from Jamplast Inc. in the form of opaque granules. Chain extender, Joncryl® 4370S, was supplied by BASF and available in the form of solid flakes with molecular weight (Mw), glass transition temperature (Tg) and epoxy equivalent weight of 6800 g/mol, 54^{o}C and 285 g/mol, respectively. OmniPur Polyethylene Glycol (PEG) 8000 was supplied by Calbiochem with a Mw of 7,000 – 9,000 g/mol to be a plasticiser in the formulation. Cloisite Na^{+} (clay) was included to improve material ductility. Ductility was an important consideration to being able to print with the prepared polymer, even though it would have been preferred to use unfilled PLA samples to more directly attribute changes in print properties to measured layer-to-layer adhesion. PLA commercial filament was obtained from a vendor located in China.

3.2 Altering the Molecular Weight of PLA

Modifying the molecular weight (Mw) of PLA was achieved by the addition of a chains extender (Joncryl® 4370S) which bridges the hydroxyl or carboxyl reactive groups of adjacent PLA chains by reaction with its multiple epoxy functional groups. Such bridging will increase the melt viscosity of PLA.

PLA granules were loaded into an internal mixer (Haake Reomix 3000P) for blending to allow for the modification of Mw by the chain extender. The capacity of the co-rotating

mixer is 310 cm^3 and was loaded with 300 g of PLA per batch with mixing temperature and rotating speed of 175°C and 75 RPM. The total resident time was 14 min, with a pre-heating and mixing time of 4 min followed by introducing the chain extender and allowed to react for 10 min. Different concentrations of chain extender were used for the formulation to obtain the different grades of modified PLA, as shown in Table **1**.

Both Clay and PEG 8000 were kept at the same concentration of 1%wt and 0.5%wt and were charged into the mixer and allowed to blend for the last 1.5 min of the process so as to have the least interference with the reaction.

Table 1: Different formulations of PLA prepared in the Haake mixer. Containing CE, PEG and clay

Sample	Conc. Of CE (wt%)	PLA [g]	CE [g]	PEG [g]	Clay [g]
1	0.200	300	0.600	1.50	3.00
2	0.500	300	1.50	1.50	3.00
3	0.750	300	2.25	1.50	3.00
4	1.00	300	3.00	1.50	3.00

3.3 Processing FDM Filament

After each batch of modified PLA was produced, the material was collected from the mixer and allowed to solidify before grinding into 2-3 mm size particles. Processing PLA into FDM filaments was one of the challenges of this study, taking into consideration the size precision, uniformity and continuity associated with processing filaments in a 3-D printer. Producing such filament via the traditional method of using a single screw extruder was not favorable due to the large output rate produced. For the purpose of this research,

extruding PLA into filament was carried out using a capillary rheometer, providing both time and cost effectiveness for processing smaller batch sizes.

The modified PLA was loaded into the capillary rheometer (Rosand RH7; Malvern Instruments Ltd) with cylindrical chamber and allowed to pre-heat for 5 min before the start of extrusion. The rheometer was equipped with an annular die(ϕ_{inner} = 2mm, ϕ_{outter} = 15mm, *l*= 32mm) to obtain the desired strand shape and size. Since the melt viscosity increased with the increase in chain extender concentration, different extrusion temperatures were used to process the different samples. A cooling and winding apparatus was developed to assure the roundness and quality of filaments was met. Ground PLA particles and the filament produced are depicted in Figure **5.**

(a) **(b)**

Figure 5:(a) Modifies PLA particles after grinding (b) Modified PLA filament

A spool wheel supplied with the 3-D printer was used in the winder. A variable voltage motor was attached to the wheel to control speed and tension applied on the filament. Half the wheel was submerged in a water bath at ambient temperature to provide the cooling

necessary. This method of extrusion proved success in providing the required dimensions standard for a FDM filament of 1.75 mm with minimal error of ± 0.03 mm.

Processing each sample of modified PLA into filaments followed trial and error methodology. Altering the processing temperature and winding speed was required to achieve optimal processing conditions. The temperature was varied between 170- 172^{o}C and the winding speed had a greater influence on controlling the diameter of the filament. The rate of winding was faster than the extrusion rate to reduce the diameter from 2 mm to target size of 1.75 mm.

3.4 Print Specimens and Parameters

For any FDM print task, there are three main stages which are drawing, slicing and communication. Drawing is performed using computer aided design software (CAD) that provide the 3D shape to be printed and is exported in (.stl) format. The drawing after is imported to a slicing software that generate the print path for the individual layers with the indicated parameters of layer thickness, temperature, print speed, fill density, etc. provided in the form of G-code. Interface software then communicates the G-code to the printer to initiate the print.

For our study, the printed sample had a rectangular shape consisting of only two layers each with the dimensions of 85 x 20 x 0.2 mm using an axial print orientation, as shown if Figure **6**. The drawing was generated using AutoCAD. Sli3er (Version 1.2.9.41) was used to select print conditions and generate the G-code. However, some manual adjustment to

the G-code was made to allow for the print of both layers at the same orientation desired instead of the normal alternating print [0, 90°] fashion. All of the print criteria and specifications are outlined in Table **2**. The G-code file is communicated to the printer using the printer host, Repetier (version 1.6.1). The printer is connected through a USB cable to the computer to initiate communication. Once the print task is sent, print nozzle and bed would heat up to the set temperatures of 185°C and 55°C, this process takes between 2-3 min for the printer in use. The printer used in the study is Prusa i3 purchased from Geeetech, with a single extrude head equipped with a nozzle of diameter 0.4 mm. Print resolution of layers and head movement precision is 0.1-0.3 mm. The maximum head and bed temperature are 240°C and 110°C respectively.

Table 2: Parameters and print conditions used for peel test printed specimen.

Print T [°C]	Bed T [°C]	Infill Density %	Fill Pattern
185	55	100	Rectilinear
P. Speed [mm/s]	**Overlap %**	**Layer Height [mm]**	**# Perimeter**
25	15	0.20	1

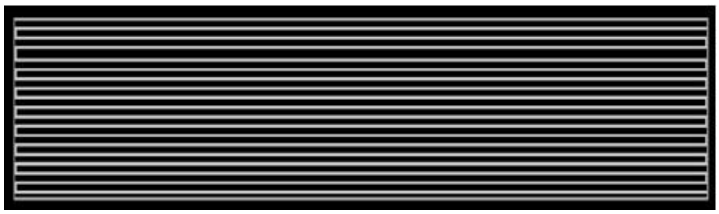

Figure 6: Bead layering orientation of printed specimen

3.4.1 Specimen Preparation Technique

Once the print had initiated and the first layer was complete, the nozzle head would go around to print the second loop layer around the specimen. While that was taking place, a strip of masking tape was placed over the last 25 mm length of the first layer and squeezed with a sharp edge tool. This would create a 25mm separation region between the two layers in the finished specimen while the remainder length of beads had direct contact between the two layers. Specimens are allowed to cool down on the heated bed (55^{o}C) for the duration of 2 min before they are removed. Detailed illustration is shown in Figure **7.**

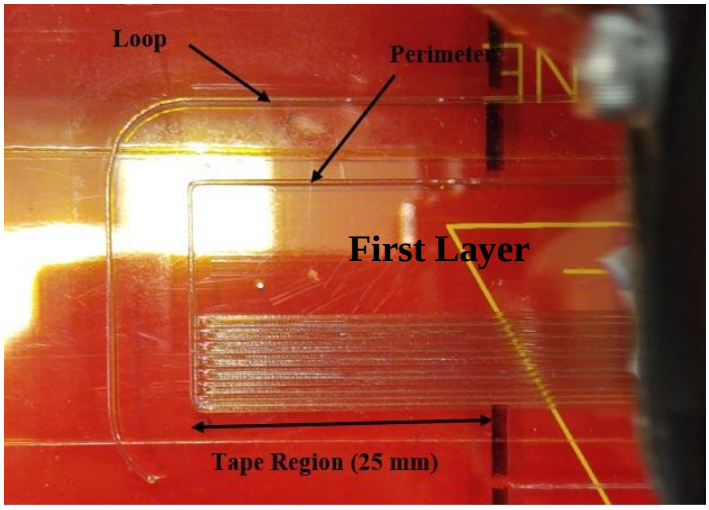

(a)

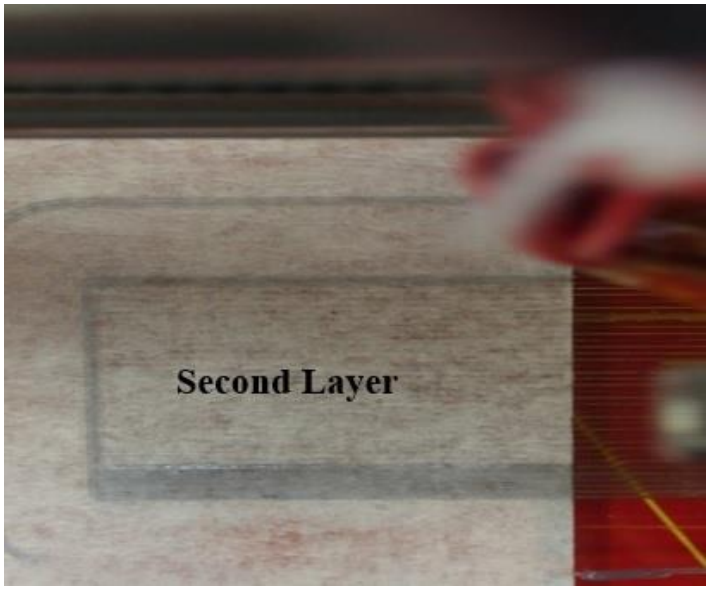

(b)

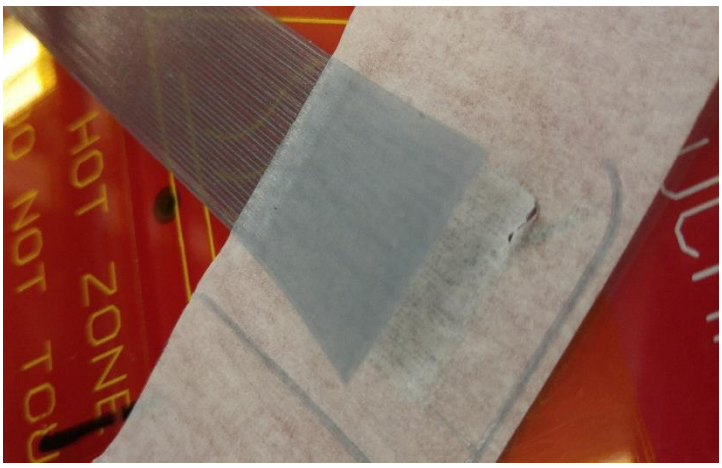

(c)

Figure 7: Preparation of specimen of two printed layers (a) first layer (b) second layer (c) complete print

Visual inspection is performed to assure the absence of defects or air-gaps between beads. The thickness of each specimen is measured at 4 locations along the interface region to verify a thickness of 0.42 mm ± 0.040 mm is achieved, see Figure **8**. Aluminum tape is

then applied from the tip of the first layer down and around to the tip end of the second layer, as shown in Figure **9.** This prevented any undesirable elongation during the performance of the peeling test, directing the peel energy to the interface between the two layers.

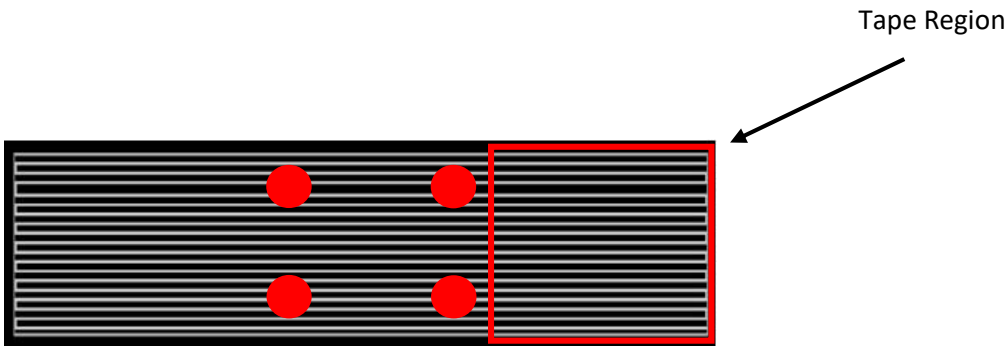

Figure 8: Illustration of the four thickness measurement locations for printed samples.

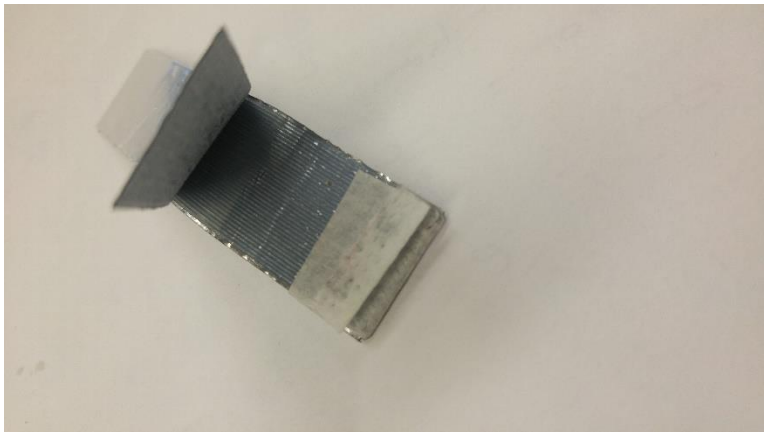

Figure 9:Aluminum tape applied on specimen to prevent elongation during peel test, photo showed is of a peeled sample.

3.5 180 degree Peel Test

The peel test was carried out on a universal mechanical tester (Instron), with load cell of 500 N. The two lips of the specimen are placed in the grips, as depicted in Figure **10**. The bottom grip is held stationary while the top grip moves at a rate of 8mm/min. The load on the grip is recorded as a function of displacement. Three successful samples were prepared and tested for each PLA grade.

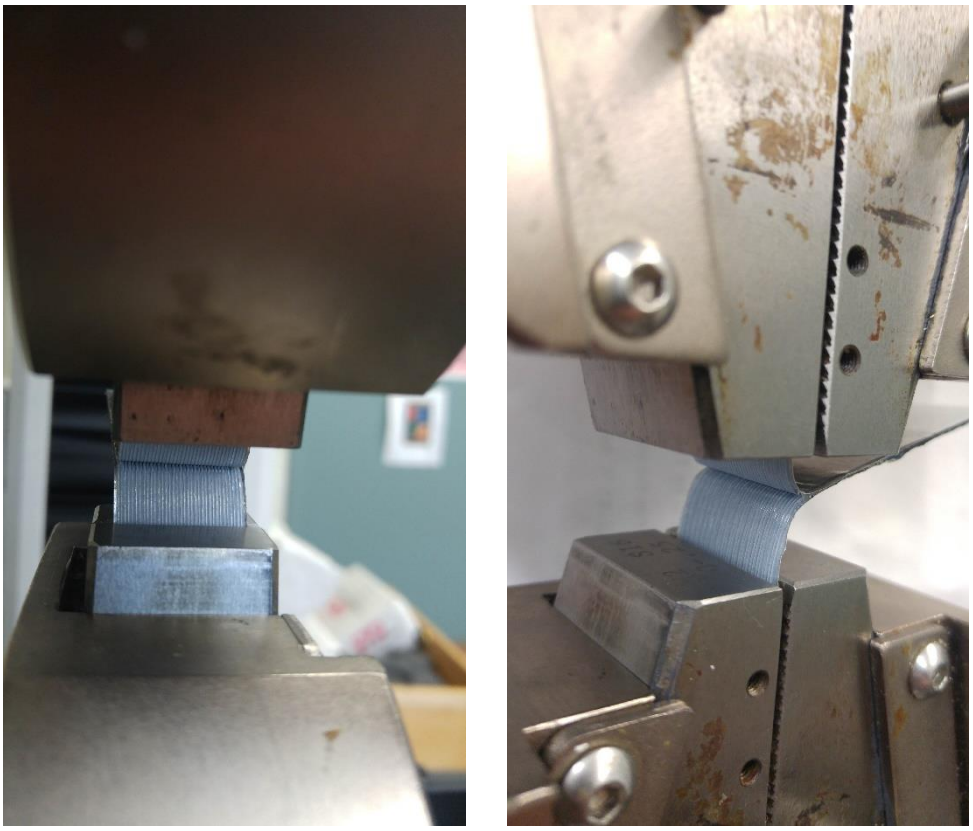

Figure 10: Peel test using universal mechanical test machine

3.6 Rheological Test

After grinding the modified PLA into small size particles, 2-3 mm, some were hot press to prepare samples for parallel plate rheometer (Ares, TA instruments) for viscosity measurement. Three test repeats were conducted for each grade of PLA produced. Results would provide a measurement for viscosity, storage modulus (G') and loss modulus (G'') for the different grades of PLA. The test was performed at T = 185°C and frequency range from 0.1 – 100 [rad/s].

3.7 Water Contact Angle

The wettability measurement of the different PLA grades for this study was obtained by telescope-goniometer method. A 1 g of each grade was hot-pressed for 5 min and allowed to cool for 6 min before the measurement was performed. Contact angle was measured after allowing the water drop to stay for 1 min on the solid surface and each grade had 4 repeats.

3.8 Differential Scanning Calorimetry

Differential scanning calorimetry (DSC) measurements were run to evaluate thermal properties of the different PLA grades, in specific, a comparison in melting temperature and melt curve. The measurements were performed on the DSC Q200 by TA Instruments. The test followed heat/cool/heat method to obtain results with no processing history, with heating rate of 10°C/min and cooling rate of 25°C/min, heating up to 175°C and cooling down to -10°C. Second test was performed on samples obtained directly from FDM, allowed to cool on heated bed for 3 min at T = 55°C and run the DSC test 5 min after the samples were first printed. Samples were cooled to -10°C and then heated to 175°C at rate

of 10°C/min. Three repeats were performed on the 1% JC for both heat/cool/heat and FDM process, error ratio was calculated based on the relative standard deviation, by dividing SD by average value of the samples and then applied the ratio across the different PLA grades.

Chapter 4 Results and Discussion

5.1 Rheology

The viscosity (η) of each batch of PLA with the different concentrations of chain extender, Joncryl (JC) at concentrations of 0.2, 0.5, 0.75, 1.0 wt.%, was determined over three repetitions for each concentration at T = 185°C and ω = 100 rad/ s , average values are shown in Table **3**. The error reported in the table and throughout this study is the standard deviation values of the samples.

Table 3: Viscosity of PLA with chain extension content

Conc. Of JC [wt.%]	0	0.2	0.5	0.75	1.0	Com. PLA
η [Pa. s]	113.41	141.79	345.31	535.96	843.52	383.44
Standard Dev. SD	12.86	33.42	55.62	127.81	58.86	46.47

A significant increase in viscosity was obtained by increasing the concentration of chain extender. This finding confirms the reaction of Joncryl with PLA and bridging the functional end groups of hydroxyl and carboxyl, which leads to an increase in molecular weight. Similar observation was concluded by (Najafi et al.[23]). The lower concentration of 0.2 wt.% JC showed little to no effect on the viscosity of PLA, which can be due to the competing reaction of thermal degradation occurring in the internal mixer. As the JC concentration increased, chain extension exceeded the observed effects of thermal degradation. An increase in molecular weight can also be concluded from the now

increasingly shear thinning behaviour as depicted in Figure 11. As JC concentration increased we observed increased shear thinning behaviour which was an indicator of longer PLA chains and more chain entanglement presence within the matrix.

The variables of storage modulus *(G')* and loss modulus *(G")* are used to characterize the viscoelastic properties of polymer melts, with *G'* describing elastic properties and *G"* describing viscous properties. We observe an increase in both *G'* and *G"* with increasing concentration of CE. *G"* remained greater than *G'* for the frequency range up to 100 rad/sec (maximum scan frequency for the rheometer) for JC concentrations of 0.2 and 0.5 wt. %, as seen in Figure 11. The cross-over point (i.e., *G'=G"*) is an indicator of more rigid structure development due to the formation of chain branching or cross-linking, which is detectable now in the case in CE concentration of 1.0 wt.%. For CE concentration of 0.75 wt.%, we nearly see a cross-over point within the shear frequency range tested. Both CE concentrations of 0.75% and 1% showed evidence of significant chain branching occurring. Viscosity testing was also performed on the PLA commercial filament, and the results are presented on Figure 12.

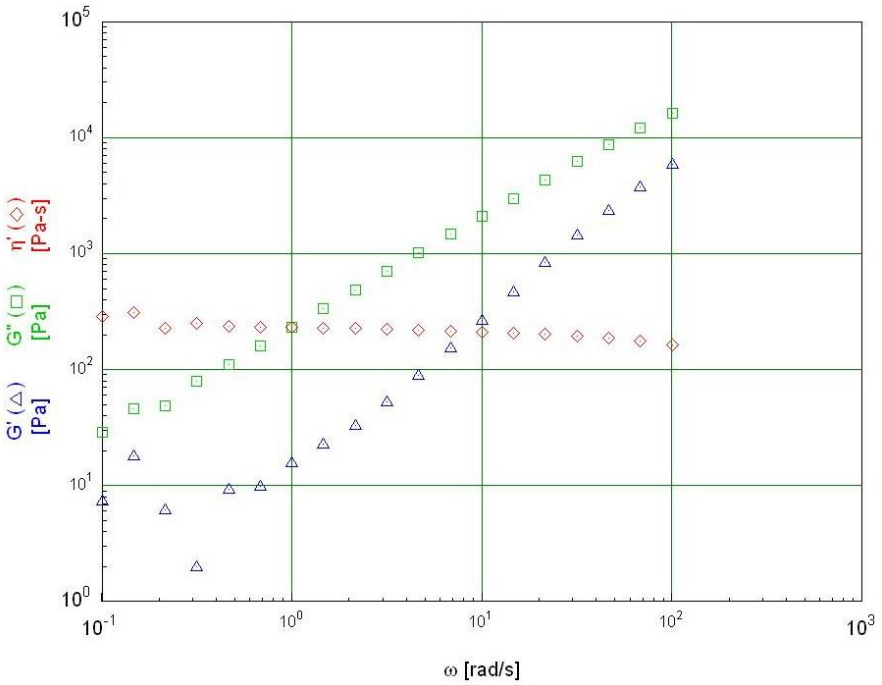

(a)

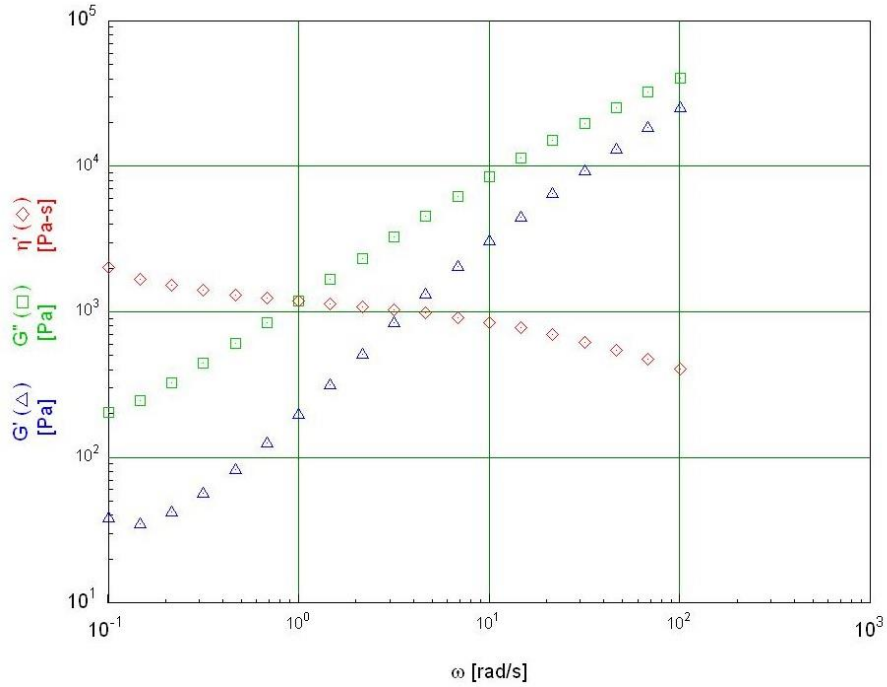

(b)

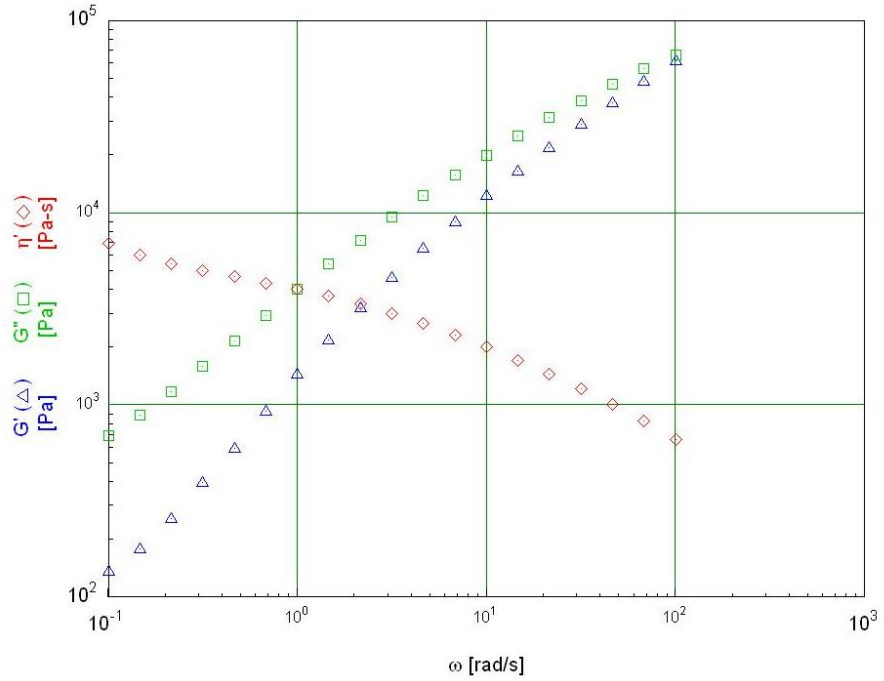

(c)

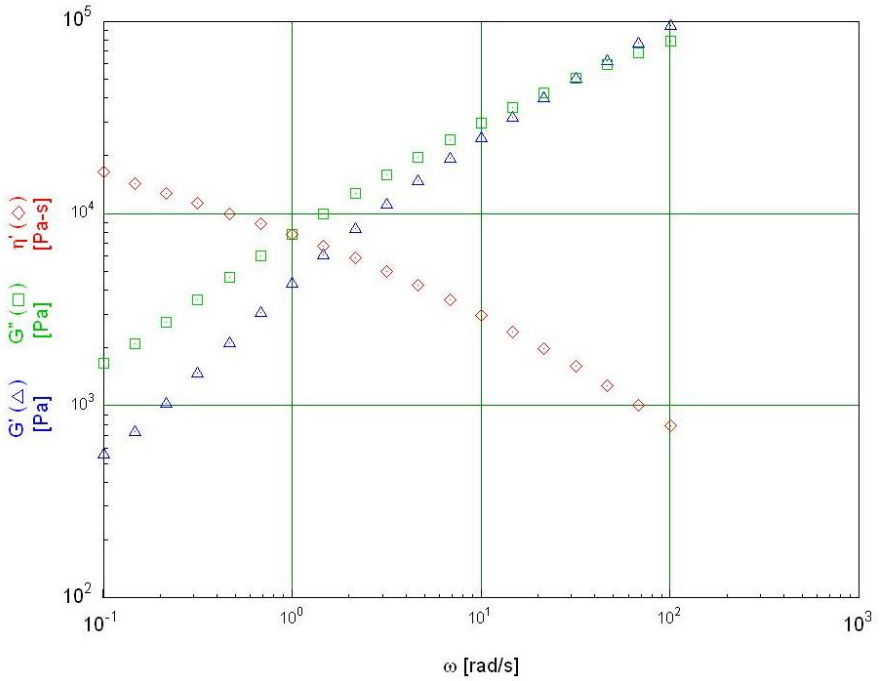

(d)

Figure 11:Parallel plate viscometer results, indicating viscosity (η) ◇, storage modulus (G') △, loss modulus (G") □ for different chain extension concentration in wt. % (a) 0.2, (b) 0.5, (c) 0.75, (d) 1.0.

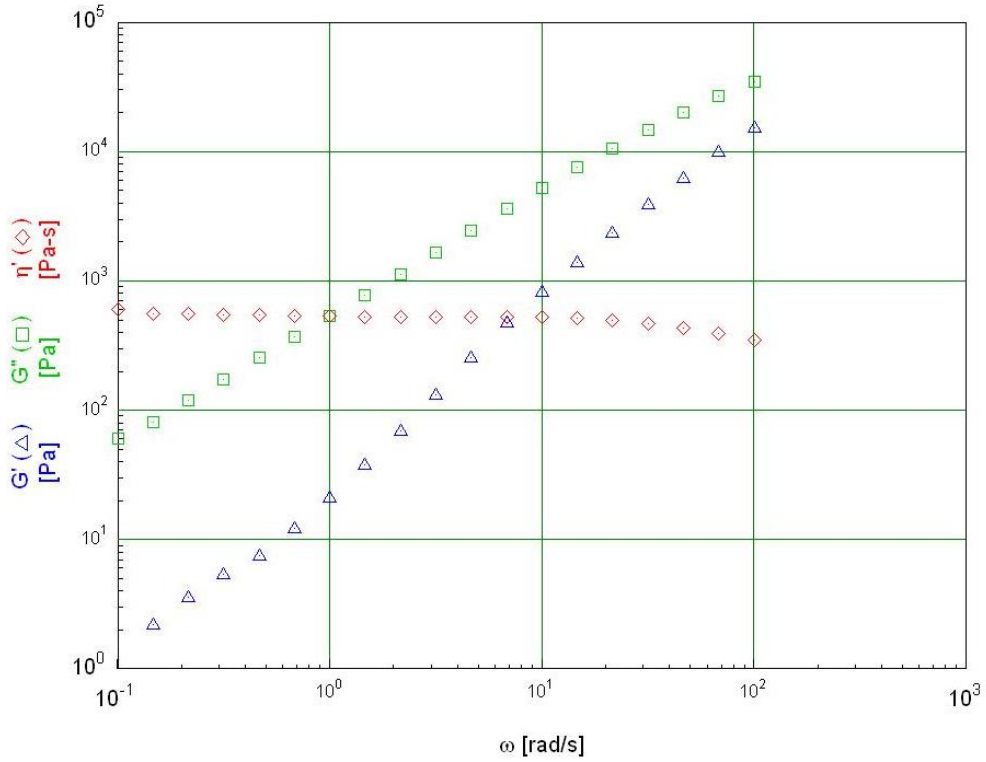

Figure 12: Parallel plate viscometer results, indicating viscosity (η) ◇, storage modulus (G') △, and loss modulus (G") □ for commercial PLA filament

5.2 Filament Extrusion

For the different grades of PLA produced, viscosity affected the melt strength of filament extruded. Due to the increase in melt viscosity, less complications were involved in producing filament with the PLA modified at CE concentration of 0.75, 1.0 wt.%. A batch of 0 wt.% CE was prepared by mixing virgin PLA in the Haake mixer along with the set concentration of clay and PEG, to obtain a reference point for the peel test and have a direct comparison. However, the sample obtained did not attain enough melt strength, which made it hard to be processed into a uniform size filament, yielding filament size below the desired thickness (i.e., 0.5 – 0.8 mm).

5.3 Peel Test

Peel tests results for the commercial PLA are shown in Figure 13. In this case, full separation of the two layers occurred, without tear or break of the beads within each layer. As can be seen from the figure, peel curves reach maximum load (~35 N) at peel initiation then slightly dropped to 28-30 N and maintained approximately the same load throughout the remaining length of the sample, as seen in Figure 13. The maximum load was selected to reflect the adhesion strength present between the two layers since the prepared resin samples were much more brittle on account of no plasticizers being added. From the results of the commercial PLA filament, we can assume the interface has approximately the same adhesion strength along the length of the sample.

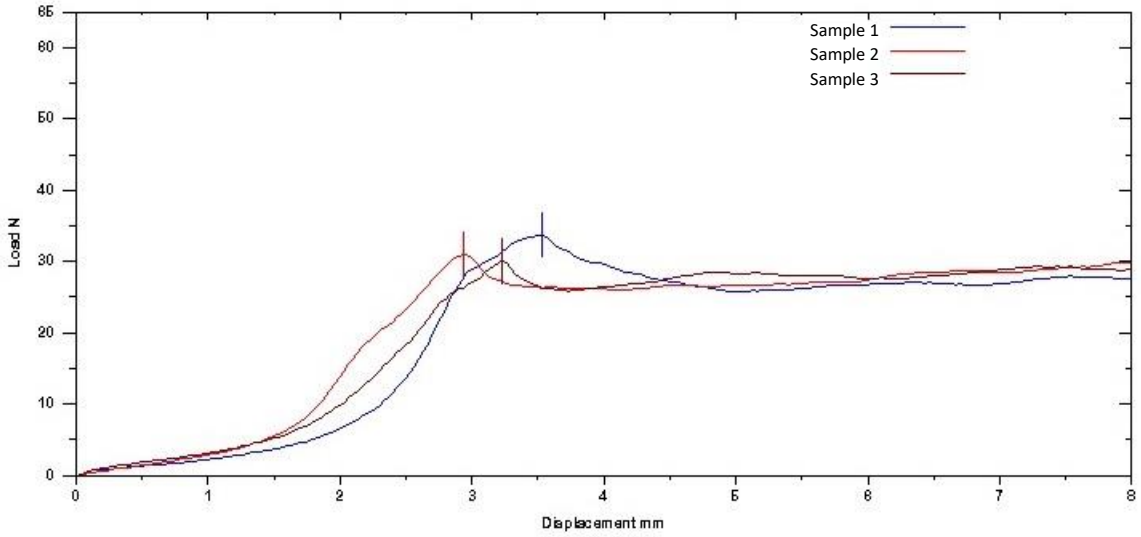

Figure 13: Peel test results of commercial PLA filament.

Results obtained by peel test for the different grades of modified PLA, produced by reaction with CE of 0.2, 0.5, 0.75, 1.0 wt.%, are shown in Figure 14. A trend of increasing strength

between layers can be seen with increasing CE concentration from the rise of load applied on each grade of PLA. Each specimen was evaluated based on the maximum load exerted on it that initiated peeling, taking place at the tip of the interface between the two layers. The average maximum load applied on the different grades of PLA with CE concentration of 0.2, 0.5, 0.75 and 1.0 wt. % are 18.26±3.90, 22.71±3.67, 35.98±7.50 and 56.74±2.22 N respectively compared to that of commercial PLA grade 31.51±3.59. The rapid drop in load exerted after reaching maximum load is due to the fail of the specimens after peel initiation; specimens formed with the more ductile commercial PLA filament showed better peel. The commercial PLA included different additives that enhanced its ductility and prevented breakage. Our developed PLA materials were prone to breakage and tearing after peel initiation.

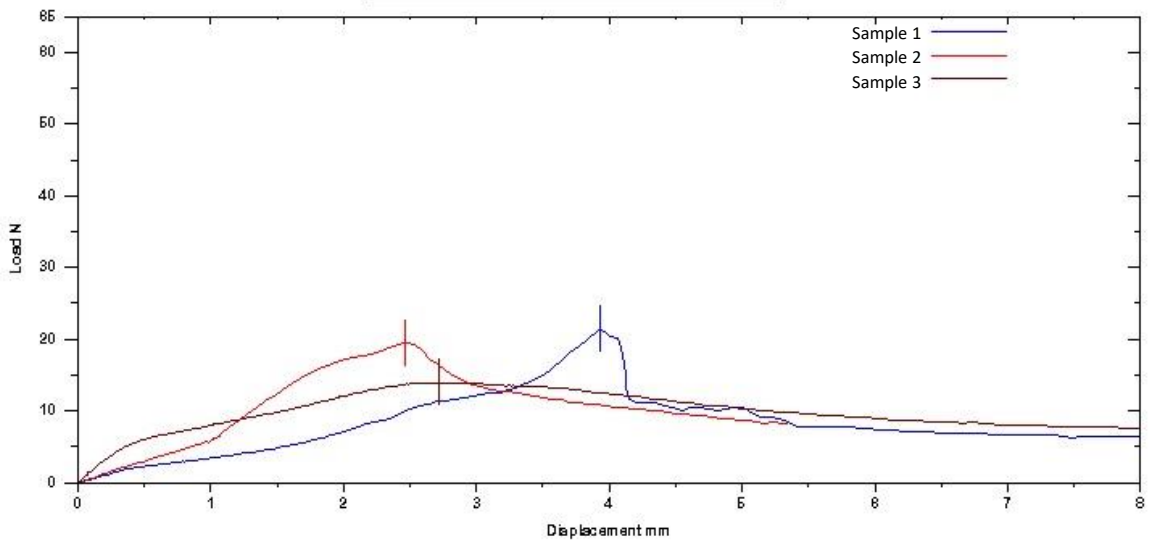

(a)

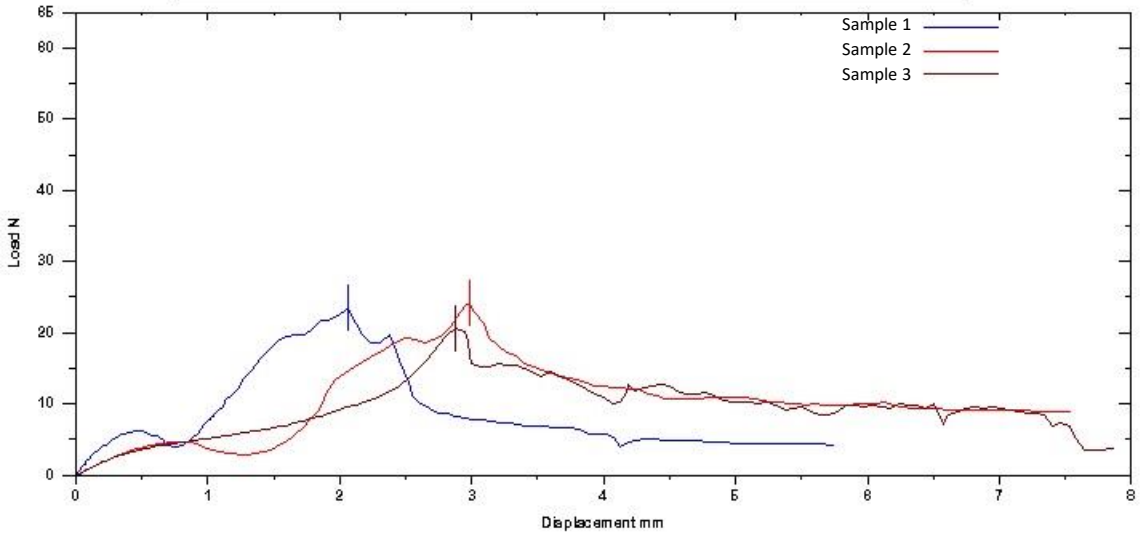
Sample 1
Sample 2
Sample 3
Load N
Displacement mm
0
10
20
30
40
50
60
70
80
0
1
2
3
4
5
6
7
8

(b)

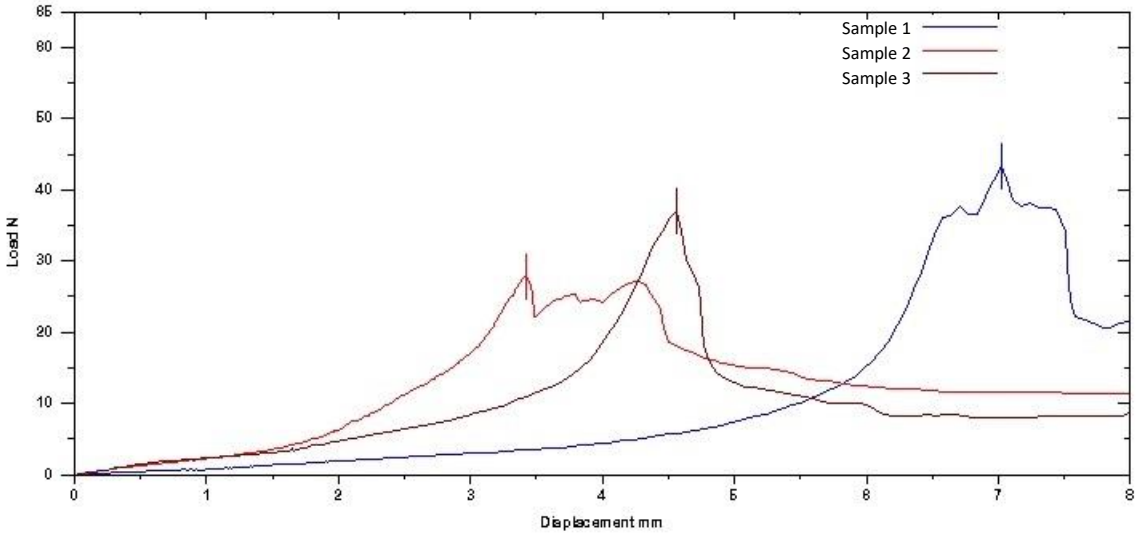
Sample 1
Sample 2
Sample 3
Load N
Displacement mm
0
10
20
30
40
50
60
70
80
0
1
2
3
4
5
6
7
8

(c)

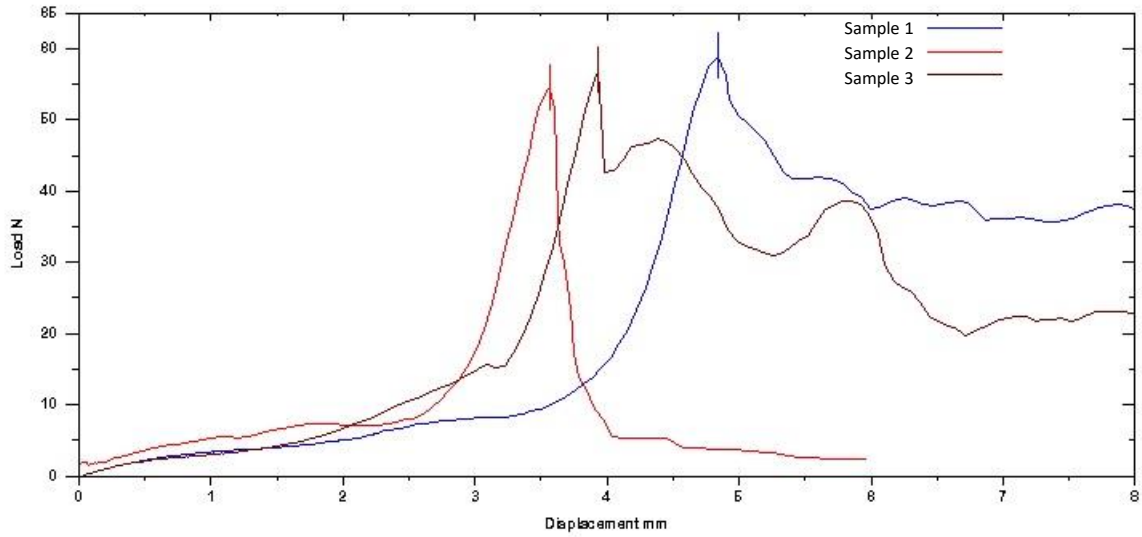

(d)

Figure 14: Peel test results of different PLA grades with CE concentration of (a) 0.2, (b) 0.5, (c) 0.75, and (d) 1.0 wt. %.

Addition of CE increased the chain length of PLA, similar to the conclusion reported by Zhong et al. [24] where PLA was reacted with the chain extender, methylenediphenyl diisocyanate (MDI). Zhong noted that a broader molecular weight distribution was obtained, which they considered as evidence of chain branching. Degree of branching was considered to be higher for higher CE concentration, based on the rheological results in our case. The increase in maximum load exerted on the interface of the peeled sample reflects an improvement in adhesion with increasing chain length. The presence of longer PLA chains would increase the degree of entanglement and branching can enhances inter-diffusion between the two layers [25].

5.4 Water Contact Angle

The gained adhesive strength seen in the peel test can arise from intermolecular associative forces or physical interactions (ex. chain entanglements and pore filling). The latter is more believed but since Joncyl is a complex chemical species, it is possible that intermolecular associations were affected. Contact angle measurement is used as an indicator of changing intermolecular forces between polymer chains, using the sessile drop technique where a drop of water is placed on top of the surface and the angle between the solid surface and liquid is measured. This measurement was conducted to investigate the possibility of a surface polarity change with increasing JC concentration in the PLA. Since the epoxy groups of Joncryl were most likely to increase hydrophilicity, water was considered a suitable fluid to test for changing surface energy. A surface is considered hydrophobic if the angle formed exceeds 90°. The results are reported in Table 4**.**

Table 4: Contact angle results for PLA with different JC concentration

Joncryl Concentration [%]				
Run	**0.2**	**0.5**	**0.75**	**1**
1	70.99	78.95	81.32	76.83
2	78.59	78.15	81.86	83.11
3	79.57	73.93	74.99	78.56
4	84.11	78.7	77.15	88.97
Average θ	**78.32**	**77.43**	**78.83**	**81.87**
δ	4.71	2.04	2.87	4.70

Surfaces that are hydrophobic usually exhibit predominant non-polar interaction with water, whereas those whose interaction with water are predominantly polar are usually hydrophilic [26].

The degree of adhesion between polymers shows the possible dependence on its polarity [25]. However, as can be seen from Table 4, there is no significant change in polarity across the different grades of PLA produced, and therefore the difference in peeling strength observed across the different PLA grades was considered to be unrelated to surface polarity.

5.5 Differential Scanning Calorimetry

Differential scanning calorimetry (DSC) measurements were run to evaluate the crystalline properties of the different PLA grades, in specific, based on a comparison in melting temperature and the features of the melt curve. The measurements were performed on the DSC Q200 by TA Instruments. DSC thermograms of the second heating cycle are shown in Figure 15.

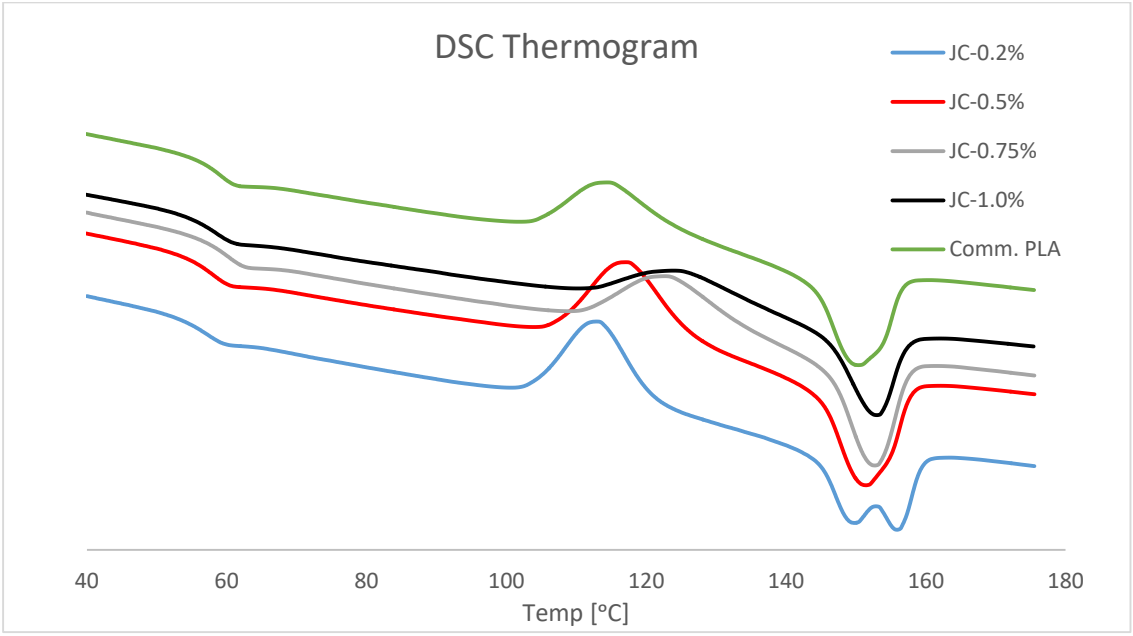

Figure 15: DSC Thermogram for the different PLA grades, presented is the second heating cycle of the heat/cool/heat process.

As seen from the figure above, there is no significant change in T_m across the PLA grades as prepared in the Haake mixer. However, there is some distinction in the shape of the melting peak that implies differences in crystal size and behaviour, notable with 0.2 wt% and 0.5 wt% CE. Endotherm of the 0.2wt% exhibits two melting peaks one at 149.84 and 155.98 ^{o}C, indicating its ability to form two main categories of different size crystals. The neat PLA (unreacted) has a T_m of 154.66 $^{\circ}$C. As the CE increases the lower temperature endotherm disappears. The enthalpy of the melting endotherm and cold crystallization for the different samples are presented in Table 5. The maximum degree of crystallization $\mathcal{X}_c$ determined without process history by the heat/cool/heat method is calculated according to Equation (2), to represent the potential to crystallize by each modified formulation.

Whereas the estimated sample crystallinity $\mathcal{X}_{cp}$ during FDM printing based on the analysis of a bead was computed using Equation (2)

$$\mathcal{X}_c = \frac{(\Delta H_f)}{\Delta H_{f,100\%}} \times 100 \qquad \text{Equation (1)}$$

$$\mathcal{X}_{cp} = \frac{(\Delta H_f - \Delta H_c)}{\Delta H_{f,100\%}} \times 100 \qquad \text{Equation (2)}$$

where ΔH_f is the enthalpy of melting, ΔH_c is enthalpy of cold crystallization and $\Delta H_{f,100\%}$ is the enthalpy of melting for a 100% crystalline polymer. The latter value is reported in literature to be 75.57 J/g for 100% crystalline PLA [27]. Determining ΔH_f and ΔH_c from the DSC thermograms involves drawing a linear baseline from the start of crystallization/ melting phase to the end of it and compute the enthalpy from the area of the endotherm.

The sample crystallinity $\mathcal{X}_{cp}$ corresponded to a second set of testing with the DSC to examine the samples taken straight from the FDM, to see whether the process had any effect on the crystals formed. Each filament grade was loaded into the printer and allowed to run the early stage of the peel test samples then paused and allowed to remain on the 55 ^{o}C heated print bed for 3 min before testing with the DSC. DSC testing began 5 min after the bead was first printed and only the results of a single heating cycle are reported. The DSC results of the different grades are presented in Figure 16 compared to the commercial resin.

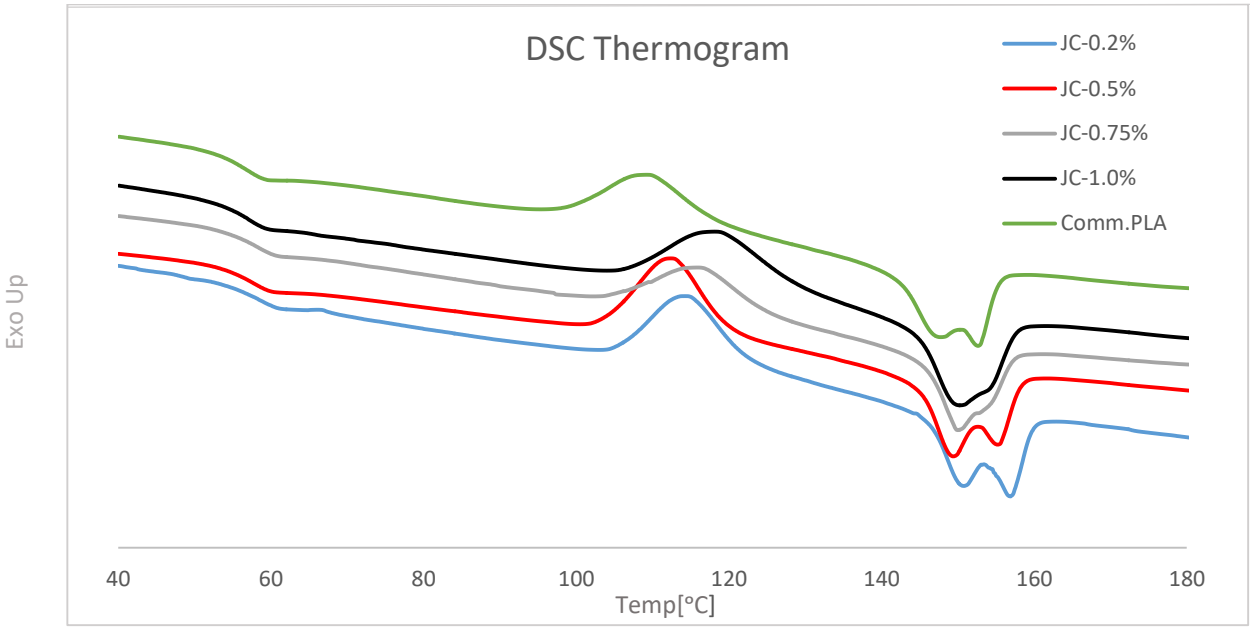

Figure 16: DSC thermogram, samples taken from FDM process and tests performed 5 min after the samples first printed. Cooled down to -10°C then heated to 180°C at (10°C/ min).

Table 5: Outlines the different thermal characterization of the varying grades of PLA from DSC thermograms

Heat/ Cool/ Heat					
Grade	**JC-0.2**	**JC-0.5**	**JC-0.75**	**JC-1.0**	**C.PLA**
T_g [°C]	57.10	57.91	60.01	58.27	58.99
T_c [°C]	113.3	117.10	122.70	123.94	114.41
T_m[°C]	149.84/155.98	151.20	152.75	152.27	150.43
ΔH_f	31.06	28.03	22.27	21.91	24.23
ΔH_c	29.37	25.94	20.98	8.87	22.31
$\mathcal{X}_c$	41.1066.85	37.0966.18	29.4764.91	27.6764.61	32.0665.34
FDM Process					
Grade	**JC-0.2**	**JC-0.5**	**JC-0.75**	**JC-1.0**	**C.PLA**
T_g [°C]	58.32	57.77	58.28	57.06	56.70
T_c [°C]	114.23	112.38	115.86	118.11	109.21
T_m[°C]	150.79/156.87	149.36/155.17	149.99	150.29	147.73/152.64
ΔH_f	31.42	28.81	27.41	25.47	28.45
ΔH_c	27.65	26.28	21.10	24.59	20.18
$\mathcal{X}_{cp}$	3.7762.78	2.5361.86	6.3164.65	1.9861.46	10.9468.06
Peel [N]	18.2663.90	22.7163.67	35.9867.50	56.7462.22	31.5163.59

The degree of crystallinity is one of the main characteristics in a polymer which determines its mechanical properties, such as yield stress, impact resistance and elastic modulus [28], and in the case of this work will determine both the brittleness of the printed sample as well as the difficulties of the next printed layer to become bonded to the lower layer. The crystallinity $\boldsymbol{x_c}$ determined for the PLA with JC concentration of 0.2, 0.5, 0.75 and 1 wt.% are 41.1066.85, 37.0966.18, 29.4764.91, and 27.6764.61% respectively. There is an effect of JC on the overall crystallinity of PLA as provided by the result. We observe a decreasing relationship of $\boldsymbol{x_c}$ with increasing CE concentration which can be due to the increase of chain branching degree and its effect in hindering crystals from forming.

The shape of the melting endotherm curves suggest a change in sizes of crystals produced in the different grades of PLA. The endotherm of sample 0.2% JC in Figure 16, shows the same two peaks as seen in Figure 15, which is indicating the presence of two types of crystals, small and larger in size. The samples of higher JC concentration with increased degree of branching, show a hindrance in the formation of larger crystals. As the JC content increases, we observe the right end of the endotherm value decreases and skewed to the left, which can mean larger crystals content has decreased. At the same time, the gap between the two sub-endotherms in the melting curve as noted in the 0.2% JC concentration decreases with increasing JC, which suggests the formation of new size crystals. Bai et al. [29] studied the crystallization kinetics of both linear and branched PLA. Their results show that the half crystallization time reduces with increasing branching degree and the overall crystallization rate are higher in branched PLA than that

in linear PLA. Even though, chain branches would hinder the formation of certain types of crystals, it was also found to act as a nucleation site which increases the overall nucleation density of the material [29].

The crystallinity χ_{cp}, for the FDM process, does not show the same overall decreasing trend of that in χ_c , however, the same observation of multiple distinguished crystal size apply, as CE increases the ability to form larger crystals decrease. The formation of the larger crystals in the 0.2 and 0.5wt. % could be attributed to the heating ramp taking place in the DSC allowing for re-orientation of crystals, not during the FDM process. The rapid cooling of the bead would allow smaller crystals to form rather than larger size crystals if any were to exist. It can be said that the degree of crystallinity has no significant impact on the adhesion strength developed between layers as seen from comparing the peeling strength with the different grades crystallinity of PLA used.

5.6 Summary of findings

The different results presented within the scope of this study are an attempt to explain the factors affecting layer adhesion in terms of the chain extender's reaction, where a change in Mw can also affect polarity, viscosity and crystallinity. We suspect the adhesion between two beads of the same type of polymer is due to chain diffusion and entanglement at the interface between the layers, which act as a bridging medium. The

↑ CE ↑ M_w ↑ η ↓X_c ↑ Adhesion

general observed effects of CE modification of PLA are:

(no change in polarity was found)

The increase of M_w resulted in chain branching with the chosen CE, as observed from the rheological results, which can increase the chances of chain entanglement. Higher Mw results in higher viscosity, thus reduces diffusivity which is the main drive of the possible entanglement at the interface and so the benefits of branching to produce the greater adhesion seen by the peel test must have arisen from a greater number of chains not bound within crystals. Degree of crystallinity did not show a significant change for FDM samples in terms of content but results suggest that size and type of crystals have reacted towards the increase of Mw and chain branching. It cannot be said for certain whether or not the type and size of crystals attributed to the improvement of adhesion strength. It is importance to note that the penetration of molecules between the two layers of printed beds should be negligibly small, as a depth of the order of 10 Å is sufficient to develop adhesion strength [24]. We assume the temperature of FDM at which PLA is printed, i.e., 185^{o}C, is sufficient to allow the mobility needed to provide the penetration required for such adhesion prior to solidification.

An increase in polarity of a polymer can lead to higher adhesion strength between layers, however, no significant change in polarity was observed across the different grades of PLA.

Chapter 5. Conclusions

The preparation of the different samples of PLA with varying concentration of CE was to understand the effect of molecular weight and chain length on the adhesion strength between two FDM printed layers. The different grades of PLA were prepared had a CE concentration of 0.2, 0.5, 0.75 and 1.0 wt% which then were processed into 3D filament with a diameter of 1.75 mm. The peeling test results of the samples obtained are 18.26±3.90, 22.71±3.67, 35.98±7.50 and 56.74±2.22 N respectively, compared to that of a commercial PLA grade, 31.51±3.59, this translate into a 200% improvement in adhesion strength. This improvement in adhesion is attributed to the increase of molecular weight achieved by the chain extender Joncryl® 4370S. The addition of CE would also result in more PLA branched chains which correlate to the increase in adhesion strength between the adjacent layers tested. We suspect the longer the branched chains, the deeper the penetration is, thus, stronger adhesion is achieved. Other possible adhesion factors such as crystallinity and polarity were examined for the different grades. While the later remained unchanged, crystallinity showed a mild decrease with increasing CE as a material characteristic, however, this change was not greatly reflected through the FDM process, thus has little to no effect on the adhesive strength developed between the layers.

Increasing the degree of branching enhance the adhesion strength through increasing the entanglement across layers which allows for stronger built for FDM parts. This material approach along with the method of testing of adhesion can be used to evaluate and compare

different materials' adhesion ability and increase the load resistance in the transverse direction of a part fabricated through FDM.

Future Recommendation

From the scope of this study it is hard to determine the type of branching introduced to the PLA chains. However, as suggested from the results, we can suspect a long-chain branch was introduced rather than a star or comb shape branch type. Controlled branching of PLA could provide more insights on the adhesion mechanism with relation to molecular weight increase. A star type branching should yield lower adhesion strength in theory compared to longer chain branching. If the diffusion theory on improving adhesion were true, and chains penetration to adjacent layers were to improve interfacial strength, then allowing longer contact duration of layers at a temperature T, $T_c < T < T_m$ should increase diffusion rate thus enhance adhesion. This requires testing in an enclosed print system with a print bed capable of providing relatively higher temperatures. Monitoring the temperature profile of the first layer by nesting thermocouples below the length of sample will provide insights about the temperature influence on the interfacial strength and chain diffusion.

References

1. B. Gross et. al," Evaluation of 3D printing and its potential impact on biotechnology and the chemical sciences", Analytical Chemistry, 2014
2. "3D Printing Speed : How Fast Can 3D printer Go? ", Jan 27, 2016 https://all3dp.com/3d-printing-speed/
3. "3D Printer Filament Guide: 25 Best Types & Comparison Charts", June 14th, 2017 shttps://all3dp.com/best-3d-printer-filament-types-pla-abs-pet-exotic-wood-metal/
4. Turner Brian N, Strong Robert, Gold Scott A. A review of melt extrusion additive manufacturing processes: 1. Process design and modeling. Rapid Prototyping J 2014;20:192–204
5. "Growth in PLA Bioplastics: A Production Capacity of Over 800,000 Tonnes Expected by 2020", June 12th, 2012 http://www.bioplasticsmagazine.com/en/news/meldungen/PLA_Growth.php
6. W. Wu, P. Geng et al., Influence of layer thickness and raster angle on the mechanical properties of 3D-printed PEEK and comparative mechanical study between PEEK and ABS, Materials 2015, 8, 5834-5846; doi:10.3390/ma8095271.
7. https://www.printspace3d.com/3d-printing-processes/
8. S. Ziemian, Tensile and Fatigue Behaviour of Layered Acrylonitrile Butadiene Styrene, Rapid Prototyping Journal, 2015
9. B. Huang et al., Raster Angle Mechanics in Fused Deposition Modelling, Journal of Composite Materials, 2015, vol. 94(3) 363-383
10. S. Ahn et al. Anisotropic Material Properties of Fused Deposition Modeling ABS, Rapid Prototyping Vol. 8. Number 4. 2002. Pp. 248-257
11. J. Christiyan et al., A study on the influence of process parameters on the mechanical properties of 3D printed ABS composite, Material Science and Engineering, V 114, 012109, pp.8, 2016.

12. S. S. Ray and M. Bousmina, “Biodegradable polymers and their layered silicate nanocomposites: in greening the 21st century materials world,” Progress in Materials Science, vol. 50, no. 8, pp. 962‑1075, 2005
13. M. H. Hartmann (1998) in D. L. Kaplan (Ed.), Biopolymers from Renewable Resources, Springer-Verlag, Berlin, pp. 367–411
14. R. G. Sinclair (1996) Journal of Macromolecular Science—Pure and Applied Chemistry A33(5), 585–597
15. H. Benninga, *A History of Lactic Acid Making*, Springer, New York, 1990
16. W. H. Carothers, G. L. Dorough and F. J. van Natta, *J. Am. Chem. Soc.*, 1932, 54, 761
17. B. Gupta, N. Revagade, and J. Hilborn, “Poly(lactic acid) fiber: an overview,” Progress in Polymer Science, vol. 32, no. 4, pp. 455‑482, 2007
18. Kazunari Masutani and Yoshiharu Kimura, Chapter 1 : PLA Synthesis. From the Monomer to the Polymer, in *Poly(lactic acid) Science and Technology: Processing, Properties, Additives and Applications*, 2014, pp. 1-36
19. D. Garlotta, A Literature Review of Poly(lactic acid), Journal of polymers and the environment, Vol. 9, No.2, April 2001
20. C. Liu, et. al, Preparation of higher Molecular Weight Poly (L-lactic acid) by Chain Extension, International Journal of Polymer Science, Volume 2013, Article ID 315917
21. H. Li, Effect of chain extension on the properties of PLA/TPS blends, Journal of applied polymer science, 122(1) p.134-141, October 2011
22. V. Frenz, et. al, Multifunctional polymer as chain extenders and compatibilizers for polycondensates and biopolymers, BASF corporation, Wyandotte, MI, USA, 2008
23. N. Najafi et al., Control of thermal degradation of polylactide (pla)-clay nanocomposites using chain extenders, Polymer degredation and sability 97 (2012) p.554-565
24. W. Zhong, Study on biodegradable polymer materials based on poly(lactic acid). I. Chain extending of low molecular weight poly(lactic acid) with methylenediphenyl diisocyanate, 1999

25. S. Voyutskii, et al., The role of diffusion phenomena in polymer-to-polymer adhesion, Journal of applied polymer science, VOL.7, PP. 475-491 (1963)
26. N. Giovambattista, et. Al, Effect of surface polarity on water contact angle and interfacial hydration structure, Department of chemical engineering, Princeton University, New Jersey, 2007
27. Kantoglu Ö., Güven O.: Radiation induced crystallinity damage in poly(L-lactic acid). Nuclear Instruments and Methods in Physics Research Section B: Beam Interactions with Materials and Atoms, 197, 259–264 (2002)
28. Y. Kong et al., The measurement of the crystallinity of polymers by DSC, Elsevier, 2002
29. J. Bai et al., Studies on crystallization kinetics of bimodal long chain branched polylactides, Royal society of chemistry, 2013.